

We are IntechOpen, the world's leading publisher of Open Access books Built by scientists, for scientists

6,300

Open access books available

171,000

International authors and editors

190M

Downloads

Our authors are among the

154

Countries delivered to

TOP 1%

most cited scientists

12.2%

Contributors from top 500 universities



WEB OF SCIENCE™

Selection of our books indexed in the Book Citation Index
in Web of Science™ Core Collection (BKCI)

Interested in publishing with us?
Contact book.department@intechopen.com

Numbers displayed above are based on latest data collected.
For more information visit www.intechopen.com



Chapter

Rheological Model of Materials for 3D Printing by Material Extrusion

Jorge Mauricio Fuentes Fuentes

Abstract

In this chapter, the viscoelastic model of Maxwell and Kelvin-Voigt and the rheological model are described. The operation and characteristic equations of a capillary rheometer are explained, as well as the Bagley and Rabinowitch corrections. Next, the method used to determine the viscosity of semicrystalline polymer is explained, using the capillary rheometer. Finally, the Rabinowitch is explained to define a rheological model that determines the viscosity of materials using a capillary rheometer.

Keywords: rheology, additive manufacturing, viscosity, manufacturing by extrusion, Bagley correction, Rabinowitch correction, cross WLF model

1. Introduction

Semicrystalline materials, such as polypropylene, are difficult to print by MEX (material extrusion additive manufacturing), due to their lack of adhesion to the print bed and their high shrinkage [1]. The problem increases when the pieces have a large surface in relation to their height, so solutions such as cellophane adhesive tapes, adhesive sprays, and other types of solutions are used. The specimens suffer evident deformations (**Figure 1**), which might affect your application. This chapter shows how a rheological study of the material is carried out to select the optimal properties that would help to mitigate the warping problem.

In this chapter, an introduction to the viscoelasticity models and rheological models is made to later carry out the study of the rheological parameters of semicrystalline polymers, which would serve as a basis for carrying out similar studies on any other polymeric material for printing by MEX.

2. Viscoelasticity

Viscoelasticity is the property that polymers must behave like an elastic solid and a viscous fluid [2]. Elastic deformation is instantaneous and independent of time. Viscous materials, such as water, resist shear flow, and they relax linearly with time when applying a strain. Elastic materials become taut when stretched and immediately return to their original state once the tension is removed. In a polymer, deformations occur with a delay in relation to the applied stresses. Polymers also have a plastic-type

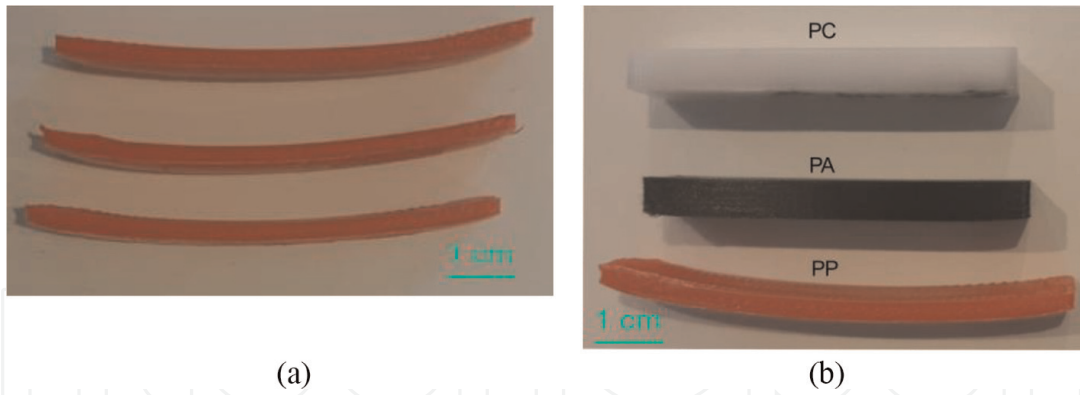


Figure 1.
a) PP specimens deformed after the printing process by MEX. b) Comparison of PP, PA, and PC specimens after the printing process by MEX.

component related to non-recoverable deformation, linked to immediate permanent deformation.

In polymers, stress and time play important parameters in mechanical behavior because they help determine if it will be strong enough, if it will be tough to withstand blows without breaking, and how the polymer will deform under load.

The response of the material is conditioned by its viscoelastic nature. The analysis of the response of these materials can be carried out from mathematical models that try to explain the behaviors, among which are:

- Maxwell's model
- Kelvin-Voight model
- Combined models.

A fully viscous response is that of a Newtonian fluid, whose deformation is linear with time while stress is applied and is completely unrecoverable.

2.1 Basic models of viscoelasticity

When there is an elastic material, the deformation (ε) is instantaneous and proportional to the applied stress (σ), which is governed by Hooke's law, shown in Eq. (1), this behavior is represented by a spring [3, 4], which represents the stiffness modulus (ξ).

$$\varepsilon = \frac{\sigma}{\xi} \quad (1)$$

For a viscous fluid, the deformation is not instantaneous and will depend on time; and this deformation is not recoverable. This deformation is represented by a plunger or piston with a fluid inside, and its behavior is given by Newton's law, according to the Eq.(2). This equation indicates that the stress or stress applied is proportional to the strain rate, whose constant of proportionality is the viscous constant of the fluid (η)

$$\sigma = \eta \frac{d\varepsilon}{dt} \quad (2)$$

2.1.1 Maxwell viscoelasticity model

This model considers that the viscoelastic model of a polymer is given by the series union of a spring and a piston. An ideal elastic element is represented by a spring that obeys Hooke's law [5, 6], with a modulus of elasticity ξ .

Since there is a series coupling of both elements, the total deformation of the assembly will be the sum of the elastic deformation independent of time (ε_1) and the viscous component (ε_2) that is dependent on time, according to the Eq. (3), see **Figure 2a** and **b**.

$$\varepsilon = \varepsilon_1 + \varepsilon_2 \quad (3)$$

On the other hand, the stresses when connected in series are equal according to the Eq. (4).

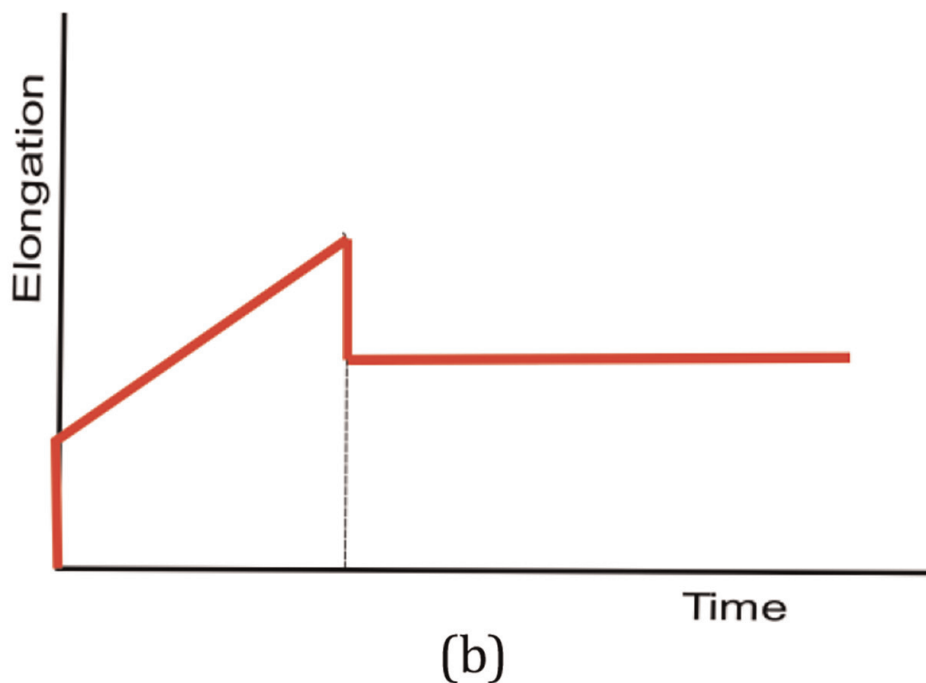
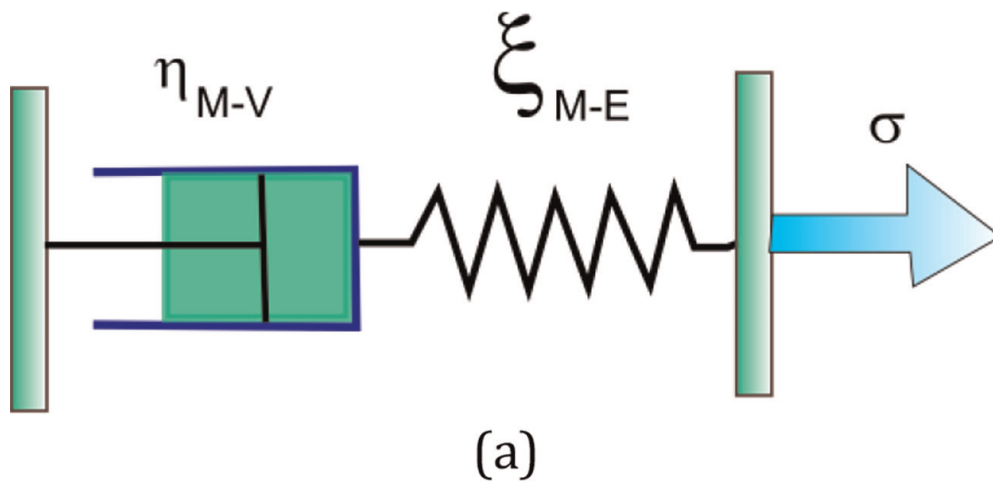


Figure 2.
(a) Diagram of Maxwell's viscoelastic model. (b) Series coupling of the elastic element (spring) and viscous element (plunger).

$$\sigma = \sigma_1 = \sigma_2 \quad (4)$$

If the time variable for the deformations is considered, the Eqs. (3) and (4) become:

$$\frac{d\varepsilon_1}{dt} = \frac{1}{\xi} \frac{d\sigma_1}{dt} \quad (5)$$

$$\frac{d\varepsilon_2}{dt} = \frac{1}{\eta} \sigma_2 \quad (6)$$

Deriving the Eq.(3) respect to time:

$$\frac{d\varepsilon}{dt} = \frac{d\varepsilon_1}{dt} + \frac{d\varepsilon_2}{dt} \quad (7)$$

$$\frac{d\varepsilon}{dt} = \frac{1}{\xi} \frac{d\sigma_1}{dt} + \frac{1}{\eta} \sigma_2 = \frac{d\varepsilon}{dt} = \frac{1}{\xi} \frac{d\sigma}{dt} + \frac{\sigma}{\eta} \quad (8)$$

If it is considered that a constant effort is applied, the expression is as indicated in Eq. (9):

$$\frac{d\varepsilon}{dt} = \frac{\sigma_0}{\eta} \quad (9)$$

Integrating the previous Eq. (9), considering that the immediate response in the elastic spring corresponds to the constant tension, we have:

$$\varepsilon = \frac{\sigma_0}{\eta} t + \frac{\sigma_0}{\xi} \quad (10)$$

It can be seen in **Figure 3** that a viscoelastic element that works at constant tension will have an immediate deformation due to its elastic component and an increasing linear deformation, due to the viscous response of the polymer.

The Maxwell model is useful when it comes to predicting instantaneous elastic deformation; however, when it comes to viscous deformation over time, it does not fit reality, since this curve is not linear.

2.1.2 Kelvin-Voigt model

In this model of viscoelasticity, the behavior of a polymer is considered as the parallel union of a piston and a spring [3, 4], as shown in the **Figure 4**.

In this model, when applying the tension, part of the energy will be stored by the spring and the rest will be slowly dissipated when the viscous element (piston) moves, resulting in a total deformation that depends on time [5, 6]. When the load is no longer applied, the original shape of the spring will recover, but not the piston, see diagram of **Figure 5**.

According to this model, the total tension applied will be equal to the sum of the tensions of the spring and that of the piston, see Eq. (11). The total deformation will be equal to the deformation of the spring and that of the piston, see Eq. (12), since they are in parallel.

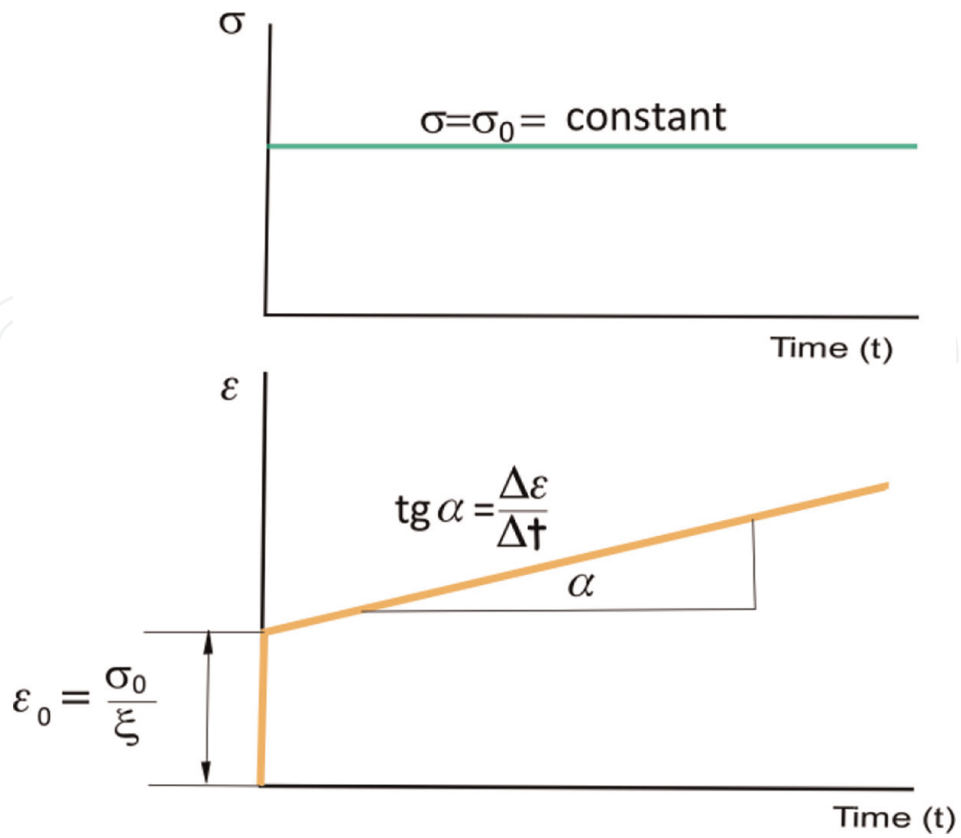


Figure 3.
 Representation of the deformation with respect to time according to the Maxwell model under the action of a constant stress.

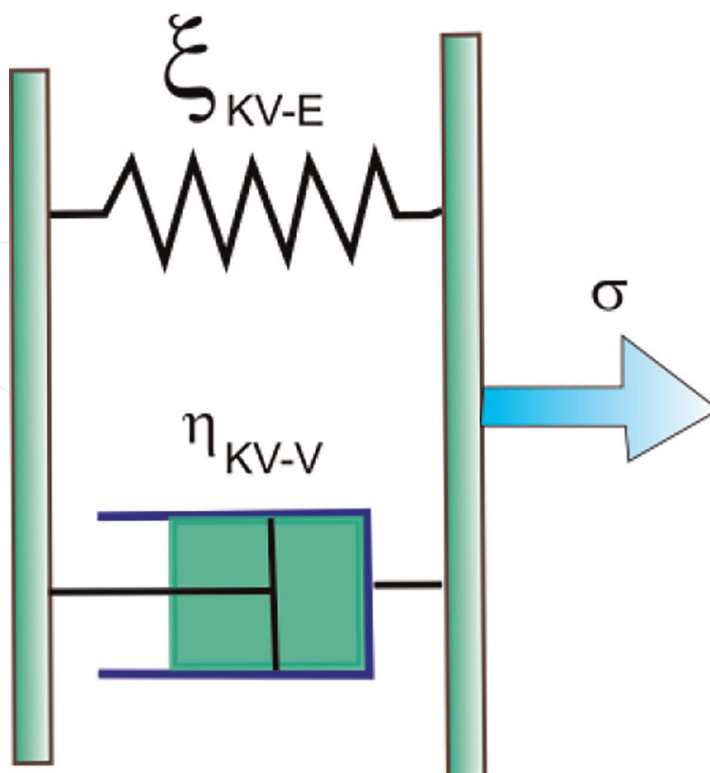


Figure 4.
 Diagram of the kelvin-Voigt viscoelastic model in which there is a parallel coupling of the elastic element and the viscous element.

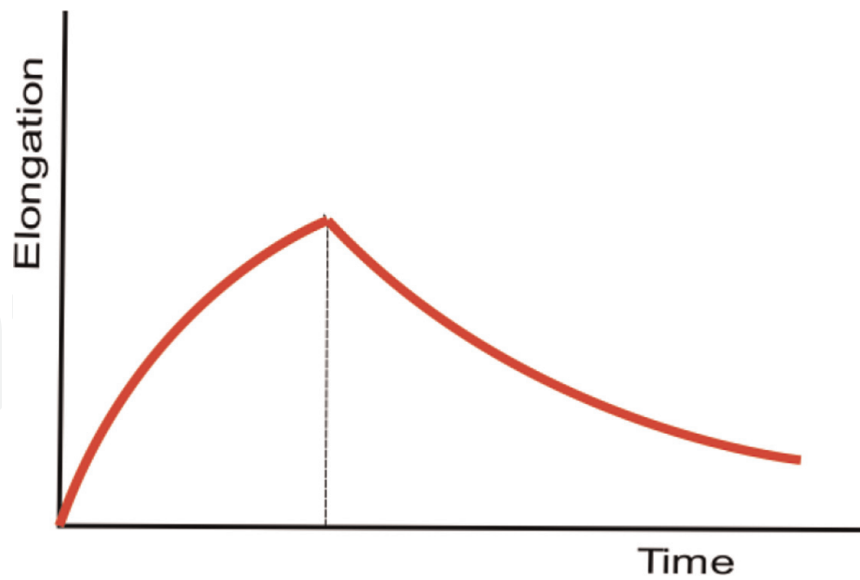


Figure 5. Diagram of the elongation that a viscoelastic element undergoes over time that complies with the kelvin-Voigt model.

$$\sigma = \sigma_1 + \sigma_2 \quad (11)$$

$$\varepsilon = \varepsilon_1 = \varepsilon_2 \quad (12)$$

Considering the addition of stresses, we have the general expression of the Kelvin-Voigt model:

$$\varepsilon = \frac{\sigma_0}{\eta} t + \frac{\sigma_0}{\xi} \quad (13)$$

$$\sigma = \xi \varepsilon_1 + \eta \frac{d\varepsilon_2}{dt} = \xi \varepsilon + \frac{d\varepsilon}{dt} \quad (14)$$

When dealing with a long-term phenomenon, we have that: $\sigma = \sigma_1 \sigma_0$, and the solution of the differential Eq. is given by the form:

$$\varepsilon = \frac{\sigma_0}{\xi} \left[1 - e^{-\frac{\xi}{\eta} t} \right] \quad (15)$$

The behavior of the polymer applying this model is shown in the **Figure 6**, in this it is observed that when a constant tension is applied to the material, it experiences a

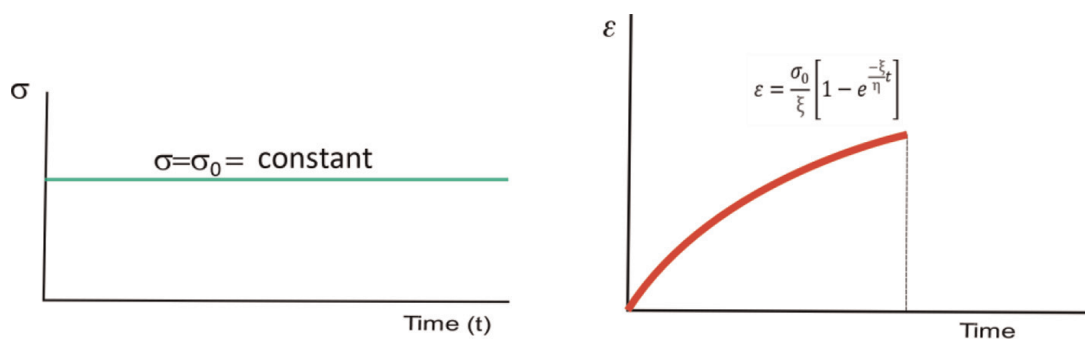


Figure 6. Representation of the exponentially deformation with respect to time according to Maxwell model.

progressive elongation exponentially. However, this does not square with reality, since at time 0, there is an instantaneous deformation.

2.1.3 Combined model (burgers)

In general terms, the Kelvin-Voigt model Eq. satisfactorily explains a real behavior such as creep, which the Maxwell model does not consider. On the other hand, the Kelvin-Voigt model does not explain instantaneous deformation (**Figure 7**), which the Maxwell model does and with a good approximation.

A good, more correct approximation that has been obtained to simulate the visco-elastic behavior of polymers is to use a combined model that considers the Kelvin-Voigt and Maxwell models and adjusts more to the real behavior, which is applicable from the point of view engineering [7]. In this model, the two models are coupled in series, according to the **Figure 8**, where the first component corresponds to the Maxwell model and the second component corresponds to the Kelvin-Voigt model.

Identifying the subscripts M to the Maxwell model, KV to the Kelvin-Voigt model, E to the elastic component of the spring, and V to the viscous component of the piston, the above equations become:

Maxwell's equation:

$$\varepsilon_M = \frac{\sigma_0}{\eta_{M-V}} t + \frac{\sigma_0}{\xi_{M-E}} \quad (16)$$

Kelvin-Voigt equation:

$$\varepsilon_{KV} = \frac{\sigma_0}{\xi_{KV-E}} \left[1 - e^{-\frac{\xi_{KV-E}}{\eta_{KV-V}} \cdot t} \right] \quad (17)$$

If the two models are considered in series, the total elongation of the system is equal to the sum of each of the Maxwell and Kelvin-Voigt systems individually. Therefore, the expression that defines the yield in the combined model is:

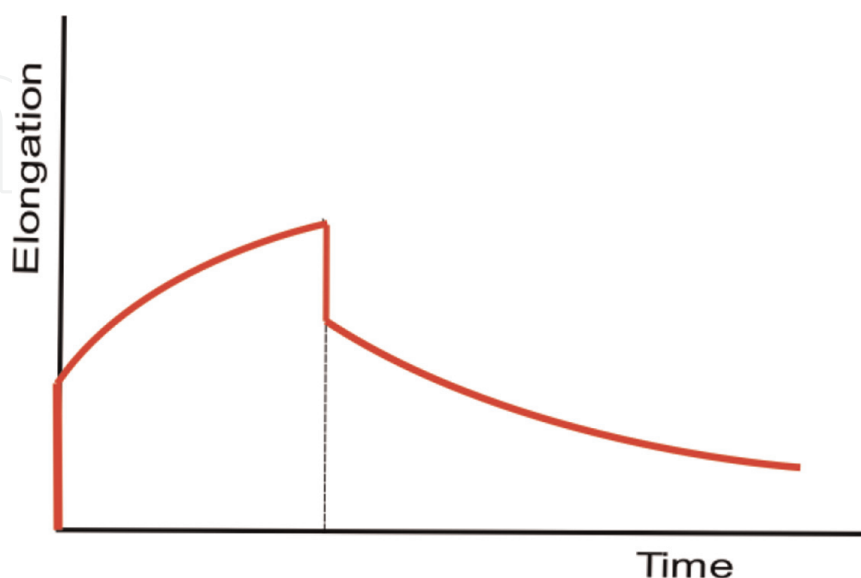


Figure 7. Schematic representation of the actual deformation that a polymer undergoes, in which the instantaneous deformation, the deformation and the viscous recovery of the material are observed.

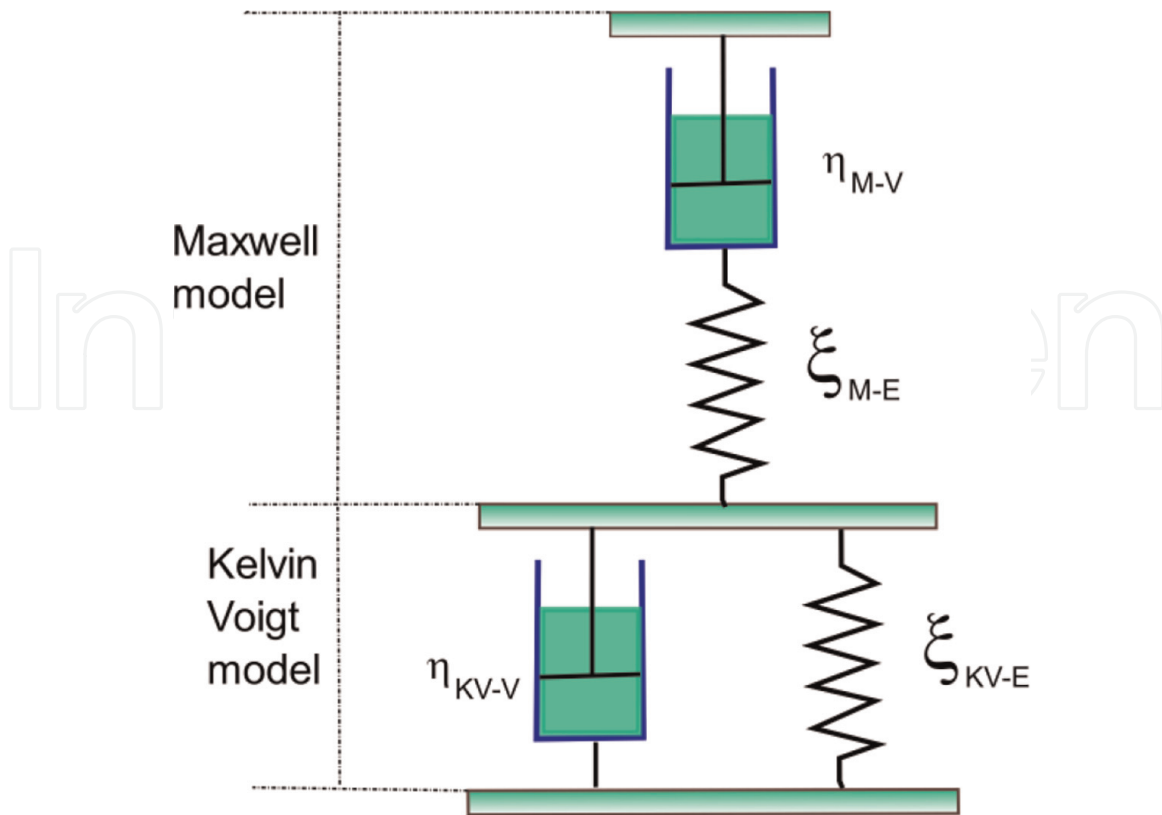


Figure 8.
Scheme of the combined viscoelastic model (Burgers).

$$\varepsilon_{\text{TOTAL}} = \varepsilon_{\text{M}} + \varepsilon_{\text{KV}} \quad (18)$$

$$\varepsilon_{\text{TOTAL}} = \frac{\sigma_0}{\eta_{\text{M-V}}} t + \frac{\sigma_0}{\xi_{\text{M-E}}} + \frac{\sigma_0}{\xi_{\text{KV-E}}} \left[1 - e^{-\frac{\xi_{\text{KV-E}}}{\eta_{\text{KV-V}}} t} \right] \quad (19)$$

Each of the terms is defined as:

$\xi_{\text{M-E}}$: Elastic constant of the spring in Maxwell's element.

$\eta_{\text{M-V}}$: Viscous constant of the piston in Maxwell's element.

$\xi_{\text{KV-E}}$: Elastic constant of the spring in the Kelvin-Voigt element.

$\eta_{\text{KV-V}}$: Viscous constant of the piston in the Kelvin-Voigt element.

See **Table 1**.

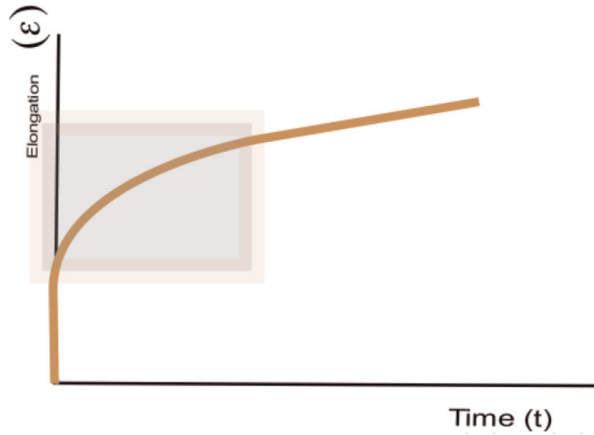
The combination of simple moldings such as Maxwell and Kelvin-Voigt allows to obtain models that are more adjusted to the real viscoelastic behavior of polymeric materials.

$$\varepsilon_{\text{M}} = \frac{\sigma_0}{\xi_{\text{M-E}}} + \frac{\sigma_0 \cdot t}{\eta_{\text{M-V}}} \quad (20)$$

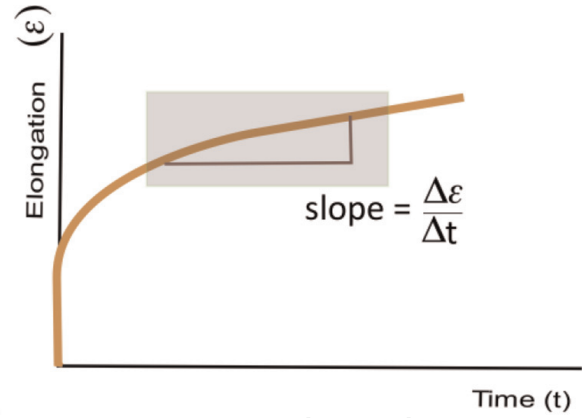
$$\varepsilon_{\text{KV}} = \frac{\sigma_0}{\xi_{\text{KV-E}}} \left[1 - e^{-\frac{\xi_{\text{KV-E}}}{\eta_{\text{KV-V}}} t} \right] \quad (21)$$

3. Polymer rheology

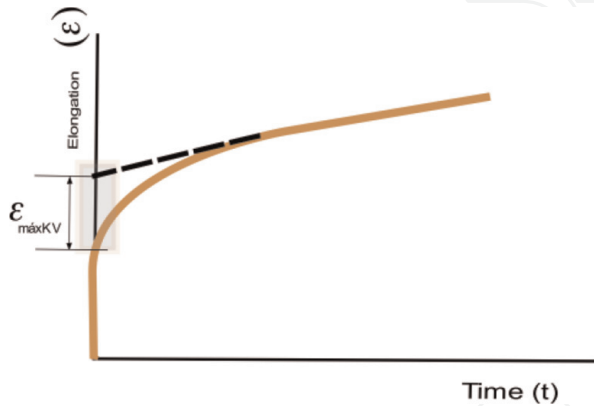
To carry out the correct modeling and simulation of the extrusion process through a nozzle for printing by MEX, it is necessary to precisely know the viscosity of the material, which depends on the physical parameters to which it is subjected [8, 9].



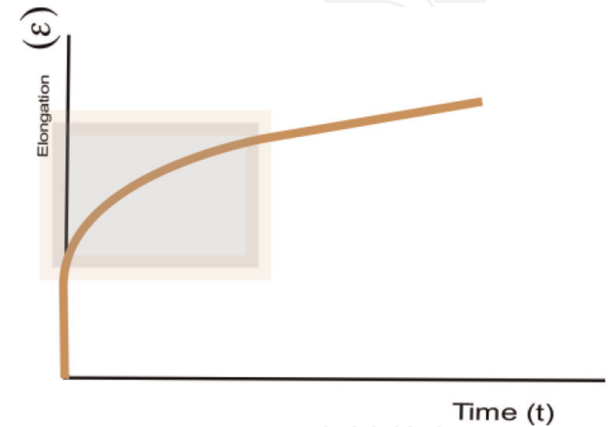
ξ_{M-E} : Elastic constant of the spring in Maxwell's element.
Interpretation:
Defines the initial deformation in the response of the combined model



η_{M-V} : Viscous constant of the piston in Maxwell's element
Interpretation:
Defines the slope of the linear yield zone after stabilization



ξ_{KV-E} : Elastic constant of the spring in the Kelvin-Voigt element
Interpretation:
Defines the slope of the linear yield zone after stabilization



ξ_{KV-E} : Elastic constant of the spring in the Kelvin-Voigt element
Interpretation:
Defines the growth rate of the exponential

Table 1.
Interpretation of the parameters of the kelvin-Voigt model in the creep curve of the material.

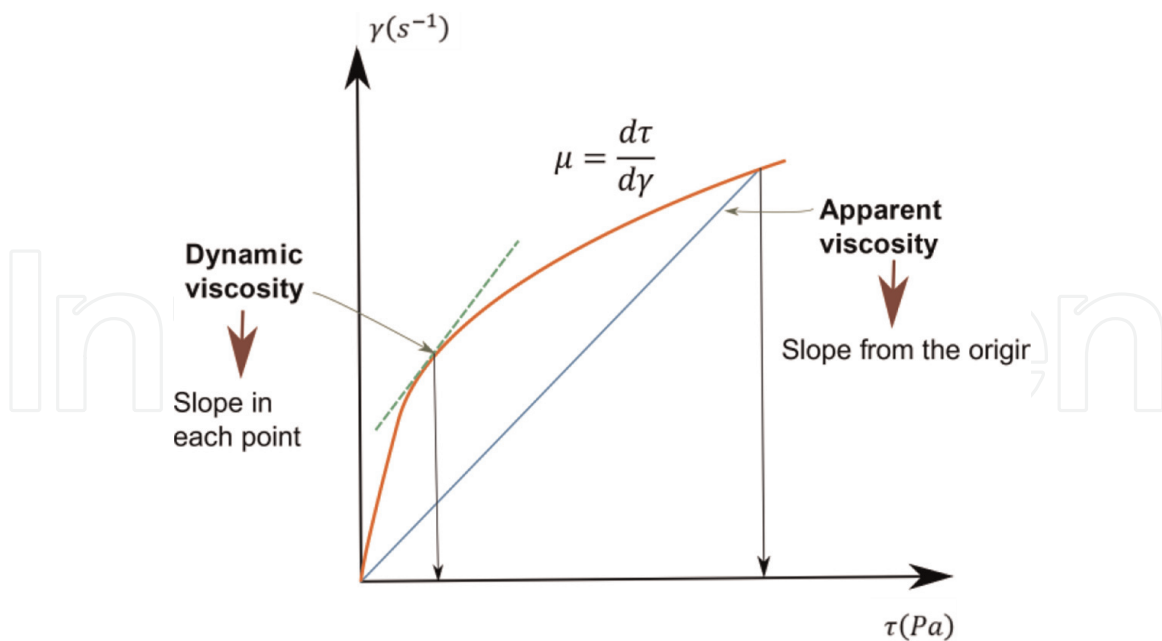


Figure 9. Diagram of the relationship between dynamic viscosity and kinematic viscosity.

There are three types of viscosity: dynamic viscosity, kinematic viscosity, and apparent viscosity. The dynamic or absolute viscosity (μ) represents the internal resistance between the molecules of a moving fluid and determines the forces that move and deform it. The kinematic viscosity (ν) relates the dynamic viscosity to the density of the fluid used and represents the resistance of a fluid to sliding. Instead, the apparent viscosity “ η ” is defined as the ratio between the shear stress (τ) and the strain rate (γ) for fluids with nonlinear behavior (non-Newtonian). If the fluidity curve is plotted (shear force vs. strain rate), it is also defined as the slope at each point on the curve, see **Figure 9**.

In **Figure 10**, the required shear stress is represented as a function of the shear speed to be reached for different liquids. In a Newtonian fluid, the slope of the curve (n) is 1, while in a dilatant fluid ($n > 1$), the viscosity increases with the shear strain rate. For some fluids such as polymer melts, some paints, and fluids with suspended particles, the viscosity decreases with increasing shear stress ($n < 1$), these fluids are called pseudoplastic or shear-thinning.

Thermoplastic polymers under low or no shear conditions behave like a Newtonian fluid, while under high shear conditions they behave like a pseudoplastic, decreasing rapidly with increasing shear rate [10], as can be seen in the example of polypropylene shown in **Figure 11**.

3.1 Rheology for 3D printing

It is necessary to know if the designed plastic will be extrudable by the MEX method, to avoid performing many time-consuming and expensive empirical tests [12], as well as avoiding nozzle clogging, setting the parameters of the 3D printing machine, as well as avoiding phenomena such as contraction and adhesion to the printing table.

To simulate plastic extrusion through the die, you can use the rheology data and compare it with a plastic that extrudes correctly and compare the rheological curves, which will show, for example, shear rate and shear stress [13, 14].

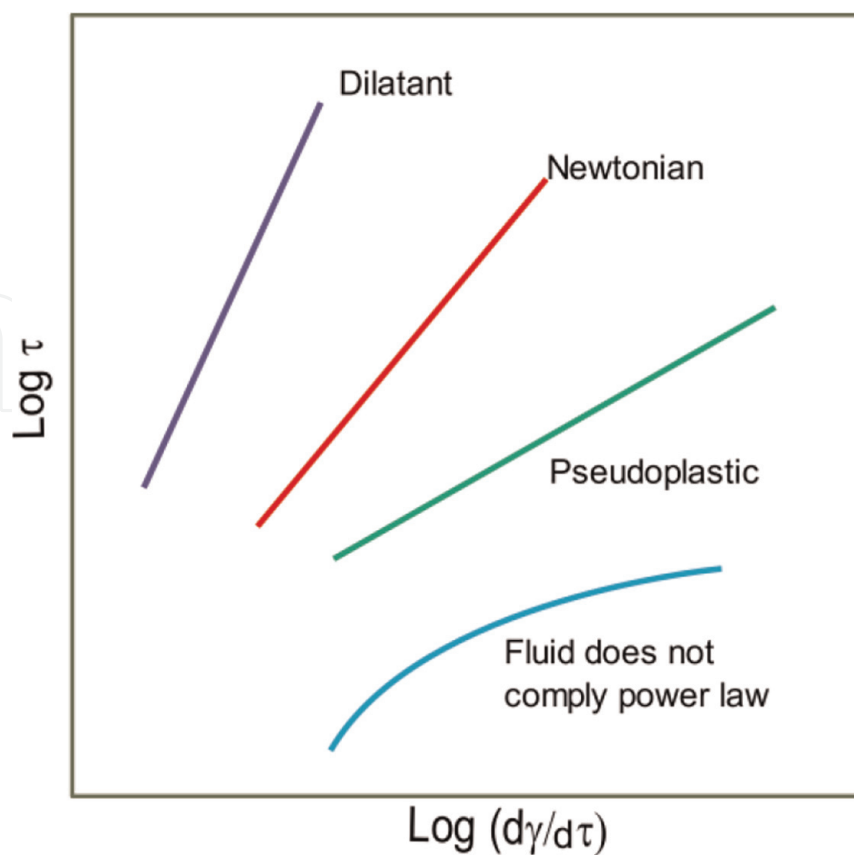


Figure 10.
 Power law schematic showing $\log \tau$ versus $\log(d\gamma/d\tau)$ for different types of fluids.

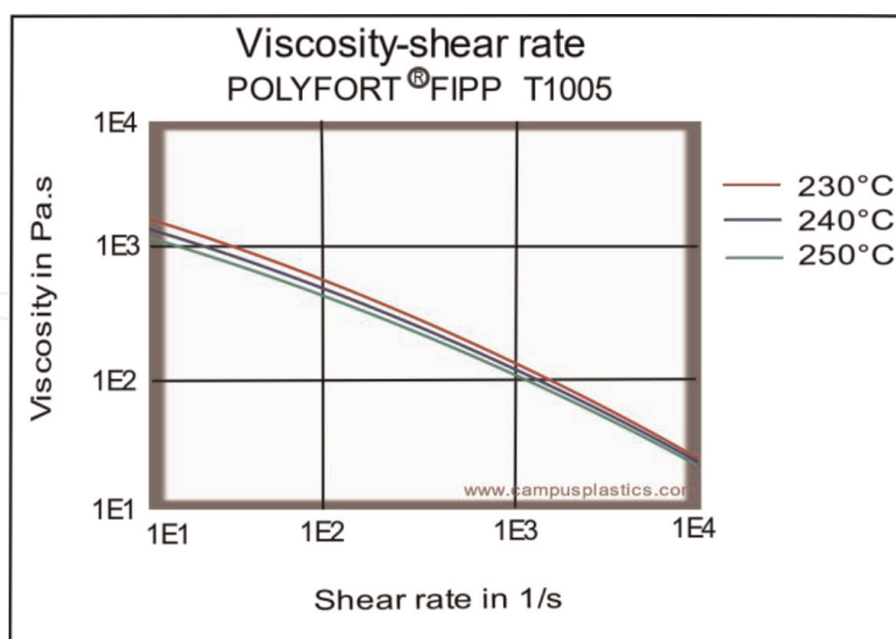


Figure 11.
 Viscosity graph of PP, POLYFORT® FIPP 30 T K1005 at 3 temperatures [11].

The cutting rate can be determined by:

- making an initial shear rate measurement of the melt viscosity to obtain the power law index.

- know the printing speed and nozzle diameter.
- apply the rheological Eqs. (1)–(4).

3.2 Viscosity measurement

One of the most important characteristics to predict the behavior of an extrusion or injection process is the viscosity of the melted material. There are several methods for obtaining viscosity as a function of shear rate [15]. Instruments used to measure shear rates must shear the fluid at measurable rates, and the stress developed must be known, for which a rotational viscometer or capillary rheometer can be used [16]. For the tests of this work, a capillary rheometer was used. Extrusion pressure or volumetric flow rate can be controlled as the independent variable, and the other is the measured dependent variable [17].

3.2.1 Rotational rheometer

In this rheometer, the fluid is sheared at a given temperature between an annular space due to the rotation of a coaxial internal cylinder inside another cylinder or by the rotation of a conical plate on a stationary plate or vice versa [18]. Rotational viscometers using two coaxial cylinders measure low viscosities of liquids, see **Figure 12a**. In a plate-and-cone viscometer, the polymer is contained between the lower plate and the cone, which rotates at a constant speed (Ω), see **Figure 12b**. These viscometers are used for viscosities less than 10 s^{-1} . This viscometer is expensive equipment, it gives information at the molecular level, and it only serves to give information about the fluid in the Newtonian regime.

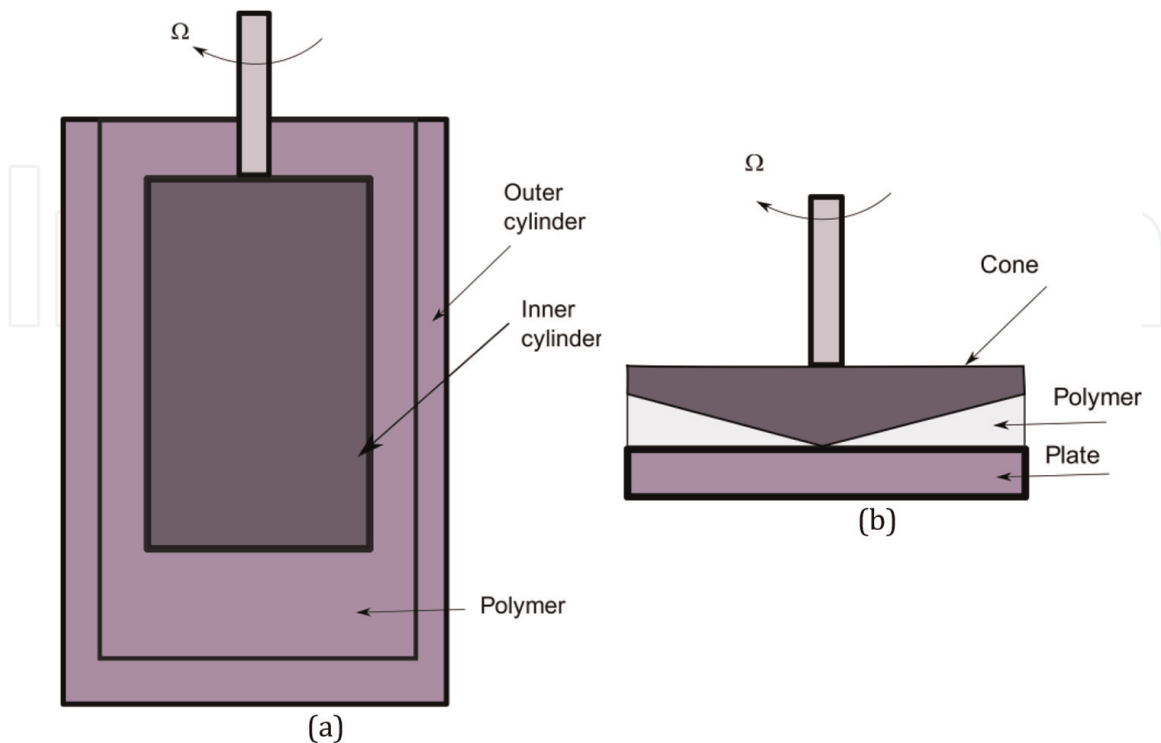


Figure 12.
a) Diagram of a coaxial cylinder viscometer. b) Diagram of a plate and cone viscometer.

3.2.2 Capillary tube rheometer

There are three main reasons why the capillary rheometer is widely used in the plastics industry [19]:

the shear rate and flow geometry in the capillary rheometer are very similar to the conditions actually encountered in extrusion and injection modeling;

a capillary rheometer typically covers the wider shear rate ranges (10^{-6} s^{-1} – 10^6 s^{-1});

a capillary rheometer provides good practical data and information on matrix swelling, melt instability, and extrudate defects.

In this equipment, the fluid is forced to pass from a container through a small diameter hole or capillary in a nozzle, by mechanical or pneumatic actuators or pistons [12]. The fluid is kept at a constant temperature due to the use of electric heating resistances (**Figure 13**).

Under constant flow and isothermal conditions for an incompressible fluid, the viscous force resisting the movement of a column of fluid in the capillary is equal to the applied force tending to move the column in the direction of flow, then:

$$\tau = \frac{R\Delta P}{2L} \quad (22)$$

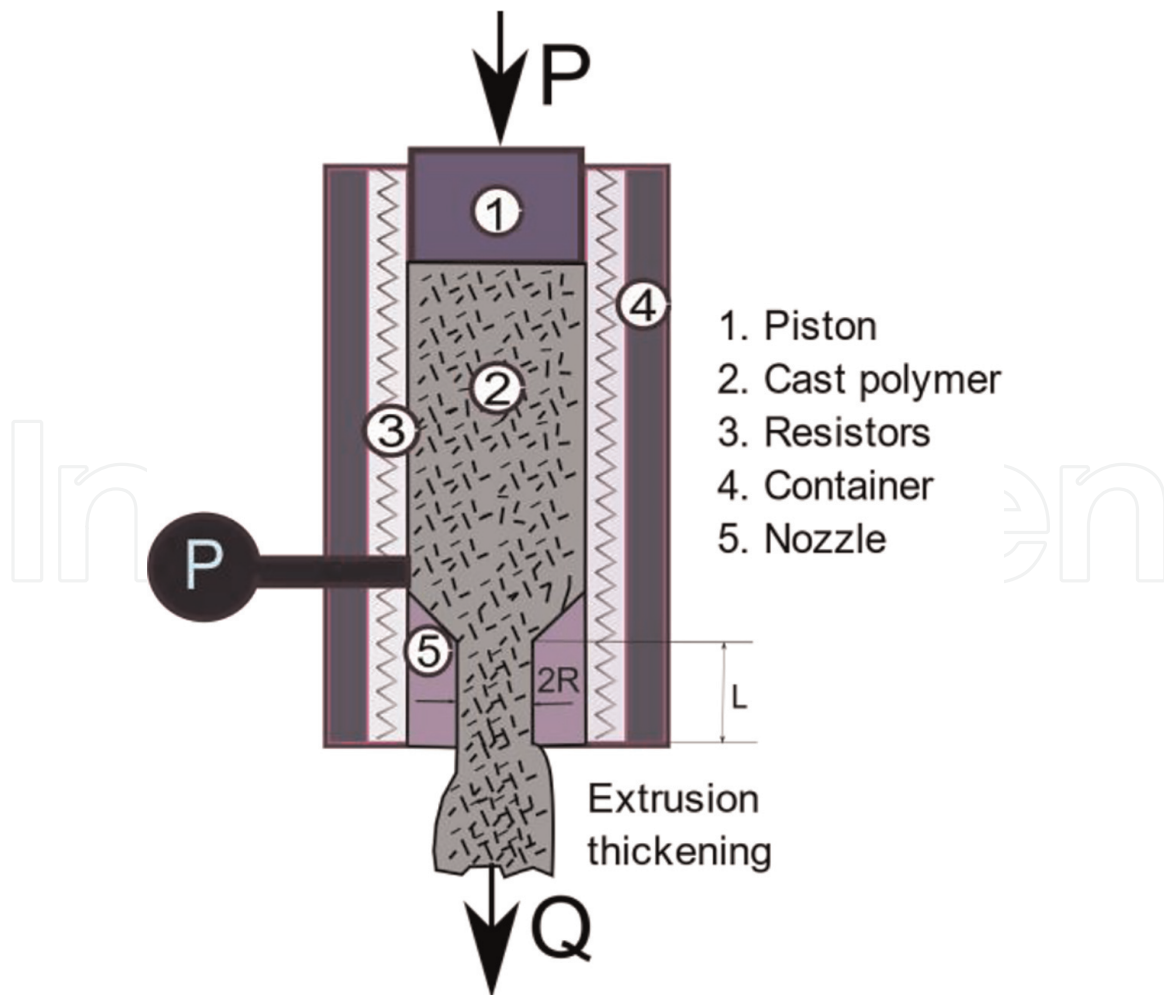


Figure 13.
Diagram of a capillary rheometer.

where,

R is the radius of the column.

L is the length of the column.

ΔP is the pressure drop across the capillary.

τ is the shear stress.

According to the above, the shear stress τ is maximum on the cylinder walls and is zero in the center. For the calculations the maximum shear stress will be used.

In normal capillary rheometry, the molten material vents to the atmosphere, and the driving static pressure in the reservoir is taken as ΔP . In such cases, end effects involving viscous and elastic deformations at the capillary inlet and outlet must be considered when calculating the actual shear stress in the capillary wall, particularly if the ratio of capillary length to radius (L/R) is small.

For a fluid that exhibits Newtonian behavior, the shear rate at the wall is given by:

$$\dot{\gamma} = \frac{4Q}{\pi R^3} \quad (23)$$

where Q is the volumetric flow rate through the capillary due to pressure ΔP , then the viscosity of the melt can be expressed as:

$$\eta = \frac{\tau}{\dot{\gamma}} = \frac{\pi R^4 \Delta P}{8LQ} \quad (24)$$

Values measured by capillary rheometers are often presented as plots of shear stress versus shear rate at certain temperatures. These values are called the apparent shear stress and the apparent shear rate at the tube wall.

3.3 Bagley's correction

This correction is applied due to the overpressure that occurs when going from a large cylinder (container or charge cylinder) to a small one (nozzle). The Bagley method is considered in which the overpressure is evaluated by relating it to an apparent increase in the length of the nozzle [20]. The total pressure drop ΔP_{tot} is given by the sum of the pressure drop in the reservoir, at the inlet ΔP_e , in the capillary ΔP , and at the outlet, due to the swelling of the polymer at the outlet. The pressure drop in the capillary is required to make the calculations and the pressure drop in the reservoir and the pressure drop at the outlet due to swelling can be neglected [21].

$$\Delta P_{\text{tot}} = \Delta P_e + \Delta P \quad (25)$$

For two or three capillaries, measurements are made of the total pressure drop as a function of the volumetric flow, for which the piston moves at different speeds, so that the flow varies, with the corresponding pressure variation, see **Figure 14**. As the flow increases, the cutting speed increases. With greater capillary length, there is a greater pressure drop.

For the same flow, the pressure drop for the three capillaries is taken. For each flow value, a minimum of 2 L/D points are obtained, and straight lines are made for each flow. In our case we have three capillaries (**Figure 15**). In total, seven flow data were taken as a function of piston speed (**Figure 16**).

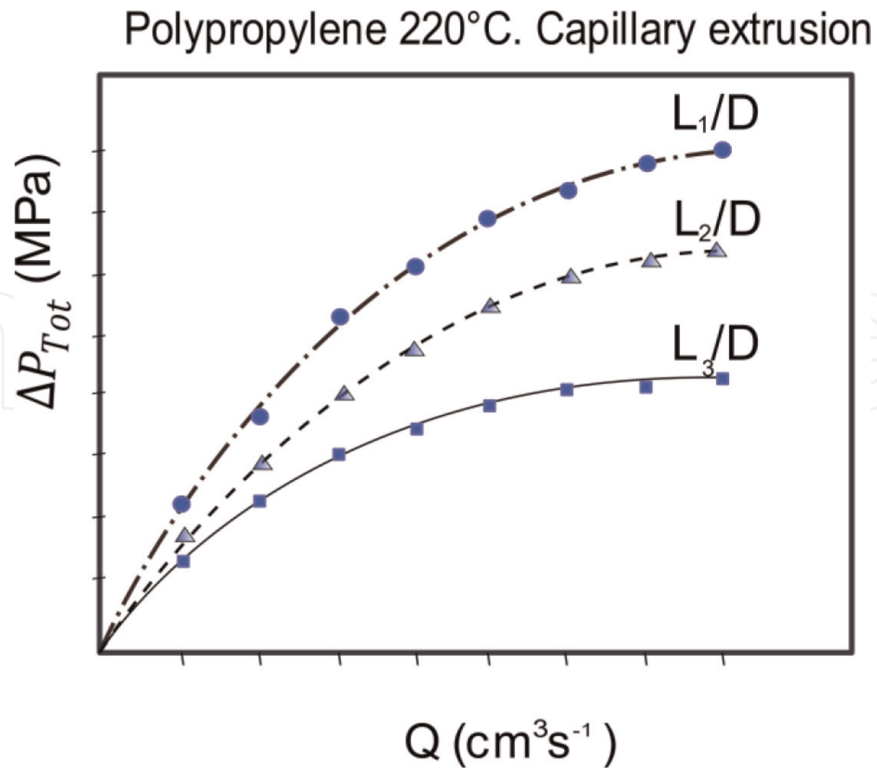


Figure 14.
 Pressure drop curve (ΔP_{Tot}) versus volume flow (Q) for three nozzles (3 L/D ratios).

The determination of the correction value is carried out with a test in which at least three nozzles with different values of the L/D ratio are used.

$$\tau_{corr} = \frac{\Delta P}{2\left(\frac{L}{R} + e\right)} \quad (26)$$

where,

τ_{corr} is the corrected shear stress in [Pa].

e is the additional apparent length of capillary measured at a given shear rate measured in [mm].

In order to determine, which is an empirical constant that tries to correct the effects of exit and entrance of material in the molten state in the capillary, it is extrapolated to $\Delta P = 0$, from the representation of ΔP versus L/D at constant shear rate and for capillaries of different lengths.

Extrapolating means that the L/D ratio is 0, that is, there is no change in diameter. When it intercepts in ΔP , the value of pressure drops at the inlet (ΔP_e) is obtained, then from Eq. 9.24 we have:

$$\Delta P = \Delta P_{Tot} - \Delta P_e \quad (27)$$

For each of the straight lines and for the three points, the shear stress is calculated corrected τ_{corr} .

The apparent shear stress is evaluated with:

$$\tau_{app} = \frac{\Delta P \cdot D}{4 * L} \quad (28)$$

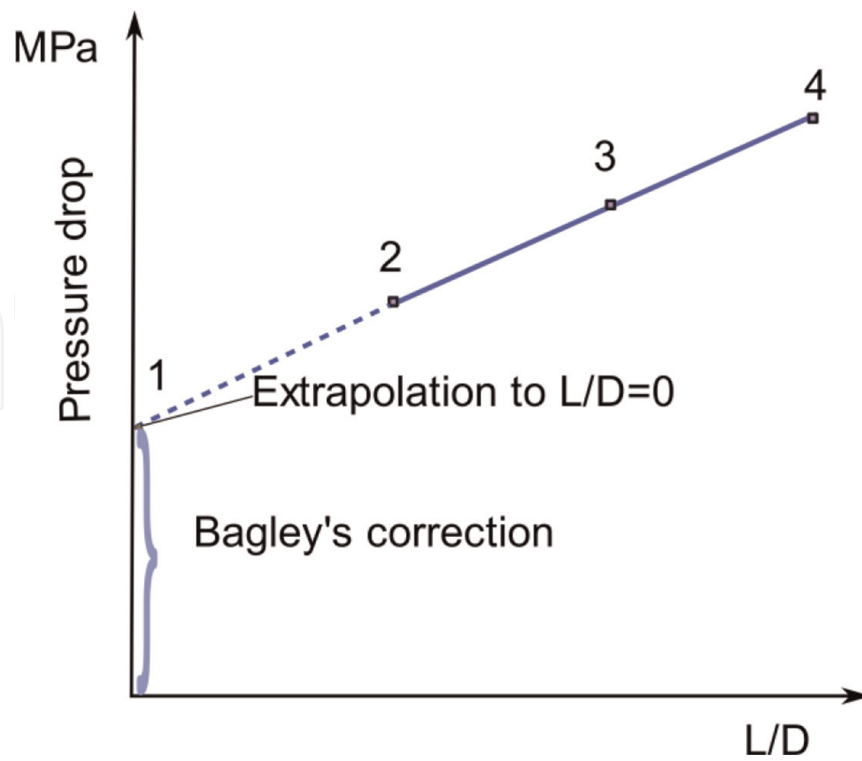


Figure 15.
Illustration of determining the value of the Bagley correction.

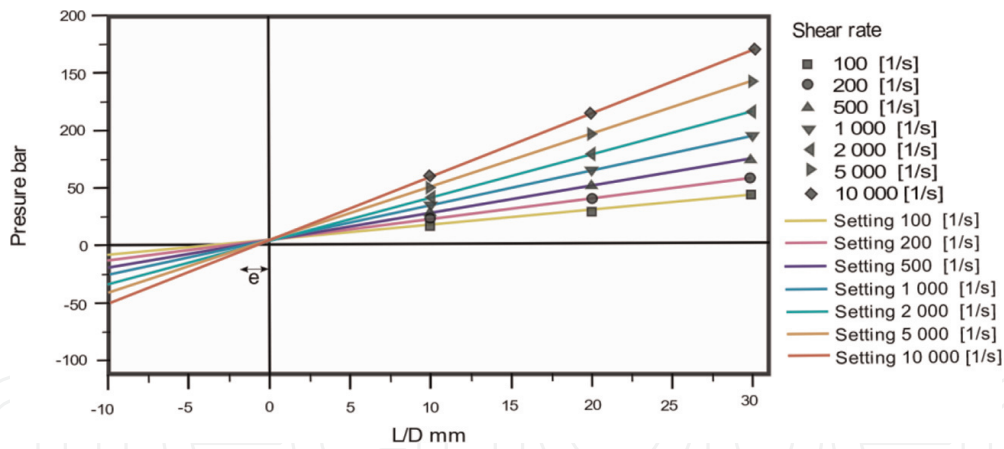


Figure 16.
Bagley plot: Pressure drop vs. L/D for different shear rates [22].

Corrected shear stress is as follows:

$$\tau_{\text{corr}} = \left(\frac{-\Delta P}{L + e \cdot D} \right) \cdot \frac{D}{4} \quad (29)$$

3.4 Weissenberg: rabinowitch correction

This correction is applied to the shear rate, since a molten plastic does not behave like a Newtonian fluid that presents a parabolic velocity distribution [23], but rather in a pseudoplastic manner, presenting a non-parabolic velocity distribution [24], this is shown in the Eq. (30)

$$\gamma_{\text{corr}} = \frac{(3 + \frac{1}{n})\gamma_{\text{app}}}{4} \quad (30)$$

where,

γ_{corr} is the corrected shear rate in [s⁻¹];

n is the slope of the relationship between shear rate and shear stress;

γ_{app} represents the apparent value of the shear rate on the tube wall;

$$n = \frac{d \log \tau_{\text{app}}}{d \log \dot{\gamma}_{\text{app}}} \quad (31)$$

n is 1 for a Newtonian fluid.

3.5 Polymer rheological models for 3D printing using Cross-WLF parameters

Cross-Williams-Landel-Ferry (WLF) model or Cross-WLF model [25] uses the results of the experimental data obtained in a capillary rheometer to describe the rheological behavior of polymeric materials, which allows the determination of their viscosity, to evaluate their processability under different conditions [26]. Within the manufacturing processes, the polymer is subjected to various shear conditions, which need to be evaluated and predicted [27]. Under conditions of low or practically zero shear, the viscosity of the material usually remains constant, presenting a Newtonian behavior. On the contrary, under high shear conditions, the viscosity decreases rapidly with the shear rate, showing a pseudoplastic behavior [28].

This model has been chosen because it can predict with a very good approximation the pseudoplastic behavior of the melt at high shear rates and the Newtonian behavior at low shear conditions [29], see **Figure 14**. This viscosity model is used in computer-aided engineering (CAE) programs such as Autodesk Moldflow™ and Ansys PolyFlow™ [30] for simulation of the plastic injection process [31, 32], because it offers the best fit to the viscosity data [33]. This model also simplifies the calculations of the pseudoplastic region, favoring the interpretation of results by considering its slope linear on a logarithmic scale [34].

This viscosity model describes the dependence of viscosity as a function of temperature (K), the shear rate T_m (γ (s⁻¹) and pressure p (Pa), which are the model dependent parameters.

The viscosity according to this model is expressed as:

$$\eta(\dot{\gamma}, T_m, p) = \frac{\eta_0(T_m, p)}{1 + \left(\frac{\eta_0(T_m, p)}{\tau^*} \dot{\gamma}\right)^{(1-n)}} \quad (32)$$

where,

η is the viscosity of the molten material in [Pa.s];

η_0 is the zero shear viscosity or the ‘Newtonian limit’ where the viscosity approaches a constant at very low shear rates [Pa.s];

τ^* is the constant of the model that indicates the shear stress from which the pseudoplastic behavior of the material begins, determined by fitting the curve [Pa] with $K = \frac{\eta_0}{\tau^*} n$ is the index of the power law in the high shear rate regime, determined by the curve fit that symbolizes the slope of the pseudoplastic behavior in the form of $(n - 1)$, see **Figure 17**.

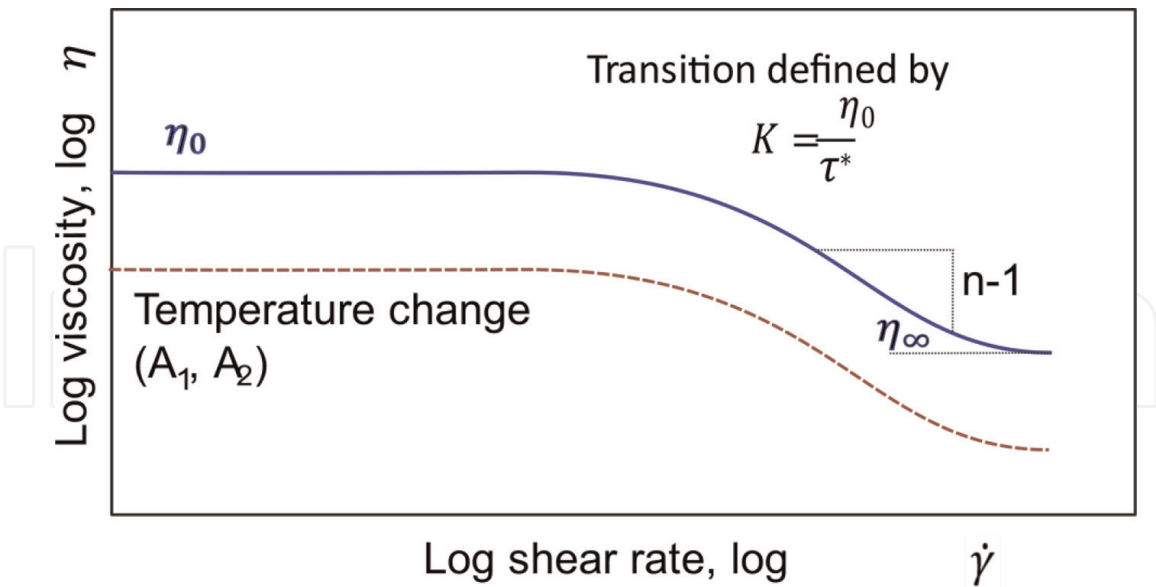


Figure 17. Approximation of the viscosity with the Cross-WLF model in Eqs. (32) and (33) [35].

$\dot{\gamma}$ is the apparent shear rate in $[s^{-1}]$.

This model is complemented by the Williams-Landel-Ferry (WLF) model. [20] which helps to determine the behavior of the material with respect to null shear phenomena and offers reliable results. His expression is:

$$\eta_0(T_m, p) = \begin{cases} D_1 \cdot e^{\left(\frac{-A_1 \cdot (T_m - \tilde{T})}{A_2 + (T_m - \tilde{T})}\right)}, & \text{si } T_m \geq \tilde{T} \\ \infty, & \text{si } T_m < \tilde{T} \end{cases}$$

$$A_2 = \tilde{A}_2 + D_3 \cdot p$$

$$\tilde{T} = D_2 + D_3 \cdot p \quad (33)$$

where:

\tilde{T} is the glass transition temperature of the material in [K], which depends on the pressure.

D_1 is the model constant that indicates the viscosity under zero shear conditions at the glass transition temperature of the material and atmospheric pressure, in [Pa.s].

D_2 is a model constant indicating the glass transition temperature of the material at atmospheric pressure, in [K].

D_3 , constant of the model that indicates the variation of the transition temperature of the material as a function of pressure, in [K/Pa].

A_1, \tilde{A}_2 , are model constants, in [-], [K], respectively.

p es the pressure in [Pa].

To use this model, its seven parameters can be determined based on estimates given by various authors [36] or by analysis of the characteristics of the materials.

4. Conclusions

It is important to know the viscoelastic and rheological properties of the materials for 3D printing by MEX, since this will allow to avoid performing an error trial

process, which is long and expensive, being able to perform the process through the necessary parameters to simulate the process through computer-aided engineering.

The rheological parameters of a polymer or composite material for manufacturing by extrusion can be determined by using a capillary rheometer, due to its high cutting speeds and shear stresses.

Bagley and Rabinowitch corrections can be applied to the results obtained through the capillary rheometer to compensate the change in diameter in the capillary, and these results can be exported to simulation programs by computer to verify the technical feasibility of manufacturing with the composite material.

When the Cross WLF model is applied, we have a good approximation of the rheological properties of the material to any pressure and temperature condition, which allows us to extrapolate the results to adjust the properties in a 3D printing process by MEX.

Acknowledgements

We thank the Central University of Ecuador for their support with time and funds to carry out this study.

Conflict of interest

The author declares no conflict of interest.

Appendix 1

Terms and symbols

$A_1 [-]$	Constant of the WLF Cross model
$A_2 [K]$	Constant of the WLF Cross model
$D [Pa \cdot s]$	Capillary diameter
$D_1 [Pa \cdot s]$	Material viscosity, under zero shear conditions, at material transition temperature and atmospheric pressure
$D_2 [K/Pa]$	Constant of the Cross-WLF model symbolizing the variation of the transition temperature of the material as a function of pressure
$\Delta P [bar]$	Constant of the Cross-WLF model symbolizing the variation of the transition temperature of the material as a function of pressure
$\Delta P_e [bar]$	Inlet pressure drop (Bagley's correction)
$\Delta P_{tot} [bar]$	Total pressure drop (Bagley's correction)
$e [Pa \cdot s]$	Additional apparent length (Bagley's correction)
$\xi_{KV-E} [MPa]$	Elastic spring constant in the Kelvin-Voigt element
$\xi_{M-E} [MPa]$	Elastic spring constant on Maxwell's element
$\dot{\gamma} [s^{-1}]$	Shear rate at which the material is being processed
$\gamma_{app} [s^{-1}]$	Apparent shear rate

η [Pa/s]	Viscosity
η_{app} [Pa/s]	Apparent viscosity
η_{KV-V} [Pa/s]	Viscous plunger constant in the Kelvin-Voigt element
η_{M-V} [Pa/s]	Viscous plunger constant in Maxwell's element
η_0 [Pa/s]	Material viscosity under zero shear conditions
L [mm]	Rheometer nozzle length
μ [Pa·s]	Dynamic or absolute viscosity
n [–]	Cross Model: Slope of the pseudoplastic behavior of the material
ν [m ² /s]	Kinematic viscosity
P [Pa]	Pressure
Q [m ³ /s]	Volumetric flow rate through the capillary due to pressure
R [mm]	Radius of capillary viscometer column
σ [MPa]	Applied stress
T [°C]	Temperature
T_m [K]	Material temperature during the Cross-WLF model process
τ [Pa]	Shear stress
τ_{corr} [Pa]	Corrected shear stress
τ^* [Pa]	Shear stress at which the pseudoplastic behavior of the material starts
τ_{app} [Pa]	Apparent shear stress
Ω [rad/s]	Angular velocity of the inner cylinder of a rotational viscometer


IntechOpen

Author details

Jorge Mauricio Fuentes Fuentes
Central University of del Ecuador, Quito, Ecuador

*Address all correspondence to: jmfuentes@uce.edu.ec

IntechOpen

© 2023 The Author(s). Licensee IntechOpen. This chapter is distributed under the terms of the Creative Commons Attribution License (<http://creativecommons.org/licenses/by/3.0>), which permits unrestricted use, distribution, and reproduction in any medium, provided the original work is properly cited. 

References

- [1] Bachhar N, Gudadhe A, Kumar A, Andrade P, Kumaraswamy G. 3D printing of semicrystalline polypropylene: Towards eliminating warpage of printed objects. *Bulletin of Materials Science*. 2020;1-8. DOI: 10.1007/s12034-020-02097-4
- [2] Hajikarimi P, Moghadas Nejad F. Mechanical models of viscoelasticity. In: *Applications of Viscoelasticity*. 2021. vol. 1. pp. 27-41. DOI: 10.1016/b978-0-12-821210-3.00003-6
- [3] Varna J, Pupure L. Characterization of Viscoelasticity, Viscoplasticity, and Damage in Composites. 2nd ed. London, UK: Elsevier; 2019. DOI: 10.1016/B978-0-08-102601-4.00016-3
- [4] Mainardi F, Spada G. Creep, relaxation and viscosity properties for basic fractional models in rheology. *European Physical Journal: Special Topics*. 2011;193(1):133-160. DOI: 10.1140/epjst/e2011-01387-1
- [5] Gutierrez-Lemini D. Engineering viscoelasticity. *Engineering Viscoelasticity*. Vol. 1. 2014:1-353. DOI: 10.1007/978-1-4614-8139-3
- [6] Fombuena V, Boronat L, Sánchez-Nácher L, García-Sanoguera D, Balart R. “Utilidad de los modelos de viscoelasticidad en el aprendizaje de la ingeniería de materiales poliméricos,” *Modelling in Science Education and Learning*. Jan 2017;10(1):137. DOI: 10.4995/msel.2017.6315
- [7] Hajikarimi P, Moghadas Nejad F. Mechanical models of viscoelasticity. In: *Applications of Viscoelasticity*. London, UK: Elsevier; 2021. pp. 27-61. DOI: 10.1016/b978-0-12-821210-3.00003-6
- [8] Mackay ME. “The importance of rheological behavior in the additive manufacturing technique material extrusion.” *Journal of Rheology*. Nov 2018;62(6):1549-1561. DOI: 10.1122/1.5037687
- [9] Polychronopoulos ND, Vlachopoulos J. Polymer Processing and Rheology. In: Jafar Mazumder M, Sheardown H, Al-Ahmed A, editors. *Functional Polymers. Polymers and Polymeric Composites: A Reference Series*. Springer, Cham. 2019. DOI: 10.1007/978-3-319-95987-0_4
- [10] Irgens F. Linearly Viscoelastic Fluids. In: *Rheology and Non-Newtonian Fluids*. Springer, Cham. 2014. DOI: 10.1007/978-3-319-01053-3_7
- [11] CAMPUSplastics | datasheet POLYFORT® FIPP 30 T K1005. <https://www.campusplastics.com/campus/en/datasheet/POLYFORT%C2%AE+FIPP+30+T+K1005/LyondellBasell/103/21818245/SI?pos=2> [Accessed: June 17, 2021]
- [12] Prabhu R, Devaraju A. Recent review of tribology, rheology of biodegradable and FDM compatible polymers. *Materials Today: Proceedings*. 2020;39:781-788. DOI: 10.1016/j.matpr.2020.09.509
- [13] Picco S et al. *Polymeric Additive Manufacturing: The Necessity and Utility of Rheology*. London, UK, London, UK: IntechOpen; 2016. p. 13 no. tourism [Online]. Available: <https://www.intechopen.com/books/advanced-biometric-technologies/liveness-detection-in-biometrics>
- [14] Carvalho C, Bom RP, Joinville C. de & Whirpool SA. Propriedades reológicas de abs e suas misturas oriundas de reciclagem primária. *Anais Do 10o Congresso Brasileiro de Polímeros*. Vol. 1. 2009:10

- [15] Maysaa M, Rahamtalla E, Deen H. Viscosity Measurement by using Melt flow Index for Thermoplastic polymers. Sudan University of Science and Technology. 2014. Available from: <http://repository.sustech.edu/handle/123456789/9099>
- [16] Morrison FA. Rheometry CM4650 Chapter 10: Rheometry. 2018. pp. 1–56
- [17] Nikzad M, Masood SH, Sbarski I, Groth A. Rheological properties of a particulate-filled polymeric composite through fused deposition process. *Materials Science Forum*. 2010;**654–656**: 2471-2474. DOI: 10.4028/www.scientific.net/MSF.654-656.2471
- [18] ASTM D 4402. Standard test method for measuring the viscosity of Mold powders above their melting point using a rotational viscometer. *Control*. 1999; **94**, no. Reapproved:5-7. DOI: 10.1520/D4402
- [19] Osswald T, Rudolph N. “Rheometry,” in *Polymer Rheology*. Munich, Germany: Carl Hanser Verlag GmbH & Co. KG; 2014. pp. 187-220. DOI: 10.3139/9781569905234.006
- [20] Bagley EB. End corrections in the capillary flow of polyethylene. *Journal of Applied Physics*. 1957;**28**(5):624-627. DOI: 10.1063/1.1722814
- [21] Dealy JM, Wang J. *Methods Melt Rheology and its Applications in the Plastics Industry*. Montreal, Canada: Springer; 2013. pp. 149-152 [Online]. Available: <http://www.springer.com/series/4604>
- [22] Montanes N et al. Modelización reológica mediante Cross-WLF de un nuevo material compuesto elaborado con bioPE y Thyme. Vol. 2. pp. 22–27, [Online]. Available: <http://revista.aemac.org/>
- [23] Pranata dkk. Study of rheological. Thermal and Mechanical Behavior of Reprocessed Polyamide. 2013;**6**(53): 679-688
- [24] M. Dees, M. Mangnus, N. Hermans, W. Thaens, A. S. Hanot, and P. van Puyvelde, “On the pressure correction of capillary melt rheology data.” *Rheologica Acta*. Feb 2011;**50**(2):117-124. DOI: 10.1007/s00397-011-0529-2.
- [25] Cross MM. Rheology of Non-Newtonian Fluids: A New Flow Equation for Pseudoplastic Systems. *Journal of Colloid Science*. 1965;**20**:417-437. DOI: 10.1016/0095-8522(65)90022-X
- [26] Ferrándiz S, Arrieta MP, López J, Navarro R. Demostració pràctica de la validesa dels models matemàtics en elements finits. Aplicació al model de Cross. *Modelling in Science Education and Learning*. 2013;**6**(3):67-82
- [27] Osswald T. Rudolf N. *Polymer Rheology: Fundamentals and Applications*. Munich, Germany: Hanser, 2015
- [28] Irgens F. Rheology and non-newtonian fluids. In: *Rheology and Non-Newtonian Fluids*. 2013;**9783319010**:1-16. DOI: 10.1007/978-3-319-01053-3
- [29] Reig MJ, Segui VJ, Zamanillo JD. Rheological behavior modeling of recycled ABS/PC blends applied to injection molding process. *Journal of Polymer Engineering*. 2005;**25**(5): 435-457. DOI: 10.1515/POLYENG.2005.25.5.435
- [30] Canonsburg TD. *ANSYS POLYMAT user ’s guide*. Knowledge Creation Diffusion Utilization. 2012;**15317** (October):724-746

[31] Debbaut B. Rheology: from Process to Simulation. 2005;**13**:23-36

[32] Acedo J. Caracterización y simulación del comportamiento viscoelástico de materiales plásticos mediante el Método de Elementos Finitos. Valencia; Spain: Universidad Politécnica de Valencia; 2019

[33] Sanchez LC, Augusto C, Helena S, Bettini P, Costa LC. Rheological approach for an additive manufacturing printer based on material extrusion. The International Journal of Advanced Manufacturing Technology. Vol. 105. 2019. pp. 2403–2414. DOI:10.1007/s00170-019-04376-.

[34] Piotr M. Numerical and Experimental Analysis of Filament-based Material Extrusion Additive Manufacturing Ph.D. thesis, Technical University of Denmark DTU, Mechanical Engineering Section of Manufacturing Engineering. 2020

[35] Ferri D, Perolo A, Nodari M. Cross-WLF parameters to predict rheological properties of polylactic acid. Annual Transactions of the Nordic Rheology Society. 2017;**25**(1):419-426

[36] Passaglia E, Martin GM. Variation of Glass Temperature With Pressure in Polypropylene. Journal of Research of the National Bureau of Standards. Section A, Physics and Chemistry. 1964 May-Jun;**68A**(3):273-276. DOI: 10.6028/jres.068A.024. Epub 1964 Jun 1. PMID: 31834721; PMCID: PMC5327688